Available online at www.sciencedirect.com
SCIENCE DIRECT®
Atmospheric Environment 40 (2006) 484–497
ATMOSPHERIC ENVIRONMENT
www.elsevier.com/locate/atmosenv

Three-dimensional pollutant concentration dispersion of a vehicular exhaust plume in the real atmosphere

J.S. Wang[a], T.L. Chan[a,*], C.S. Cheung[a], C.W. Leung[a], W.T. Hung[b]

[a]*Department of Mechanical Engineering, Research Centre for Combustion and Pollution Control, The Hong Kong Polytechnic University, Hung Hom, Kowloon, Hong Kong*

[b]*Department of Civil and Structural Engineering, The Hong Kong Polytechnic University, Hung Hom, Kowloon, Hong Kong*

Received 22 September 2004; received in revised form 6 July 2005; accepted 23 September 2005

Abstract

The pollutant dispersion process from the vehicular exhaust plume has a direct impact on human health, particularly on vehicle drivers and passengers, bicyclists, motorcyclists, pedestrians and people working nearby. A three-dimensional vehicular pollutant dispersion numerical model was developed based on the Reynolds-averaged Navier–Stokes equations coupled with a $k-\varepsilon$ turbulence model to simulate the initial pollutant dispersion process of carbon monoxide, CO, from a vehicular exhaust plume in the real atmospheric environment. Since the ambient wind direction and velocity are stochastic and uncontrollable in the real atmospheric environment, a wind-direction–frequency-weighted (WDFW) approach was used to obtain the real pollutant concentration dispersion along with the development of the vehicular exhaust plume. Within the specified sampling period, the ambient windflow conditions are transformed into the corresponding frequencies of wind directions and averaged magnitudes of wind velocities from directions N, E, S or W. Good agreement between the calculated and measured data for two diesel-fuelled vehicles indicates that with the WDFW approach the initial dispersion of pollutant concentration from a vehicular exhaust plume in the real atmospheric environment can be truly reflected. The present study shows that the dispersion process in the near region for the relative concentration of CO, from $R_C = 0.1$ (or 10%) to 1 (or 100%), is less influenced by the ambient wind velocity than by the vehicular exhaust velocity, but it is vice versa in the far region from $R_C = 0$ (or 0%) to 0.1 (or 10%). It implies that the effect of vehicular exhaust exit velocity on the dispersion process is more pronounced than that of ambient wind velocity at the vicinity of the exhaust tailpipe exit, while the effect of ambient wind velocity gradually shows a significant role for the dispersion process along with the development of a vehicular exhaust plume.

Keywords: Vehicular exhaust plume dispersion model; Carbon monoxide; Wind-direction–frequency-weighted (WDFW) approach; Numerical simulation

1. Introduction

Motor vehicles are the major source of air pollutants in most densely populated urban cities. There are substantial literatures describing the methods for modelling of vehicular exhausts in the

*Corresponding author. Tel.: +852 2766 6656; fax: +852 2365 4703.
E-mail address: mmtlchan@inet.polyu.edu.hk (T.L. Chan).

1352-2310/$ - see front matter © 2005 Elsevier Ltd. All rights reserved.
doi:10.1016/j.atmosenv.2005.09.046

atmosphere (Sharma and Khare, 2001), modelling air quality in street canyons (Vardoulakis et al., 2003) and showing the comparison and evaluation of several mobile-source and line-source models (Marmur and Mamane, 2003). Among these different-scale environments, the dispersion process from the vehicular exhaust plume has a direct impact on human health, particularly on the vehicle drivers and passengers, bicyclists, motorcyclists, pedestrians and people working nearby in roadway microenvironments. As the ambient wind direction and velocity are stochastic and uncontrollable in the real atmospheric environment, the physics involved in the pollutant concentration dispersion of a vehicular exhaust plume in the vicinity of roadways becomes more complex in nature. Although many empirical models (e.g. the Gaussian and K theory dispersion models) have been widely used to assess the pollutant concentrations of urban road environments due to traffic vehicles, they can only provide the gross averaged predictions. Flow structures such as the eddy variation or turbulence characteristics are difficult to be revealed.

In order to reproduce the qualitative features of airflow and pollutant concentrations from a vehicular exhaust plume near field region, limited two- or three-dimensional Reynolds-averaged Navier–Stokes (RANS) equations and pollutant transport equations including the turbulence models have been proposed. Fraigneau et al. (1995) simulated a two-dimensional pollutant (nitrogen oxides, NO_x) dispersion process near the motorway which was coupled with the reaction of nitric oxides and ambient ozone. The interaction between the turbulence and chemical reaction was calculated within the local scale of 200 m in the vicinity of the motorway. A two-dimensional pollutant dispersion numerical model was developed based on the joint-scalar probability density function (PDF) approach coupled with a k–ε turbulence model to simulate the initial dispersion process of NO_x, temperature and flow velocity distributions from a vehicular exhaust plume (Chan et al., 2001). A three-dimensional numerical model coupled with a k–ε turbulent closure was developed for simulating the dispersion of carbon dioxide, CO_2, from a heavy-duty diesel truck exhaust plume (Kim et al., 2001). The previous studies used a fixed/main dominant wind direction in their numerical calculations. In the present study, it is intended to apply the numerical models to the near-field region of initial dispersion behaviour of the pollutant plume emitted from a vehicular exhaust tailpipe. This type of pollutant dispersion not only has a direct impact on human health, but also constitutes a major fraction of the total pollutant dispersion (Venkatram et al., 1999).

Hence, the aim of the present study is to develop a three-dimensional numerical model based on the RANS equations coupled with a k–ε turbulence model using the commercial FLUENT code and a wind-direction–frequency-weighted (WDFW) approach to simulate the initial dispersion process of CO distributions from a vehicular exhaust plume. This numerical model will then be validated by comparing the calculated CO concentration with CO data measured in situations that represent the vehicle behaviour in the crowded roads of most Asian cities. The simulated situations include vehicles at both low idle (when vehicles stop due to the congested road traffic or at red traffic light) and high idle (when vehicles start moving in response to the change of traffic light from red to green) conditions.

2. Experimental description

To validate the developed numerical model, two diesel-fuelled vehicles, namely, a taxi (vehicle A) and a light-duty van (vehicle B), were used in the present study. The experimental set-up is shown in Fig. 1 in an open environmental area. In the experiment, the selected test vehicles were not moving but their engines were running at low and high idle conditions in order to simulate the situations of vehicles stopping at the red traffic light in a low idle condition during the congested traffic, and in a high idle condition during the change from red to green traffic light. Location 0 represents the exit conditions of a vehicular exhaust tailpipe. Nine

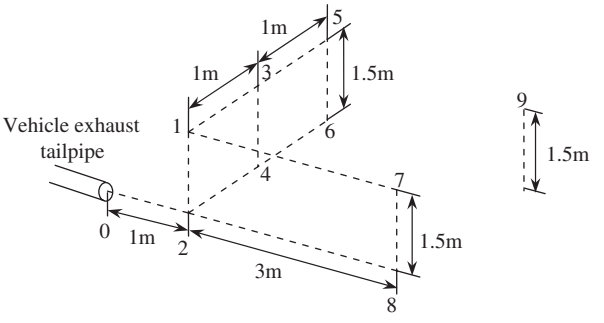

Fig. 1. Configuration of a vehicular exhaust plume and experimental set-up. (Points 0–8 are the CO sampling locations, and point 9 is the meteorological and background CO sampling location).

sampling points (1–9) were chosen along the vehicular exhaust plume with the x-, y- and z-axes representing the streamwise, lateral and transversal directions, respectively, as shown in Fig. 1. The conditions of the vehicular exhaust tailpipe exit are taken as one of the inlet boundaries in the whole computational domain. The locations 1, 3, 5, 7 and 9 approximately simulated the breathing level of human body at 1.5 m above the ground level. The locations 2, 4, 6 and 8 were at the same height along the centreline of a vehicular exhaust plume in streamwise and lateral directions. Location 9 represents the meteorological and ambient background conditions, which is far from the pollutants of the vehicle exhaust plume. Measured values at the vehicular exhaust tailpipe exit and ambient conditions are given in Table 1. In the present study, the CO pollutant was chosen for studying the pollutant concentration dispersion process from a vehicular exhaust plume because its chemical transformation is relatively slow in the atmosphere. The corresponding concentrations of CO were collected using sampling bags (points 1–9) and analysed using the gas filter correction CO analyser (Model 48, Thermo Environmental Instruments Inc., USA). The concentrations of CO at location 0 were analysed using the CO analyser (Model 300 NDIR, California Analyser Instruments Inc., USA). The temperatures at location 0 were measured using the thermocouple data logger (Model TC-08, Pico Technology Company, UK). The velocities at location 0 were measured using the anemometer (Model AM5000, Airflow Development Ltd., UK). The local ambient weather conditions were monitored using the combined wind velocity and direction sensors, temperature and humidity sensors and the data acquisition device (Models DNA022, DMA570 and BSA020.E, LSI Spa, Italy) close to location 9. In the present study, the sampling data of local ambient wind velocity and direction, temperature and relative humidity were taken at every 10 s, 1 min and 10 min intervals, respectively. The total sampling period was 4 min for both low and high idle modes.

3. Mathematical model description

3.1. WDFW approach

The local ambient wind directions and velocities are complex in the real atmospheric environment. The general approach is either to use the wind tunnel experiment to simulate the ambient windflow pattern or to assume the ambient windflow in a fixed or a specified direction, which cannot truly reflect the heterogeneous windflow characteristics (Kim et al., 2001; Chan et al., 2002a). However, it is vital that the pollutant dispersion along with the development of a vehicular exhaust plume on near-field region and its response to the local ambient flow field be known for representative wind velocities and directions for such short time and distance scales. The vehicle-based pollution has not only a direct impact on human health, but also constitutes a major fraction of the total pollutant dispersion (Venkatram et al., 1999). Hence, a transformation approach of real local ambient wind direction is used in the present study. In general, the ambient wind velocity could be transformed into 8 or 16 directions for most empirical Gaussian models that are used to predict the variation of long-term (i.e., month or year) averaged pollutant concentration along the downwind distance according to the meteorological wind velocities and directions of the wind rose diagram. Niemeier and Schlunzen (1993) used a three-dimensional mesoscale model to study the flow patterns around the island for eight different geostrophic wind directions.

However, the interested computational domain in the present study for solving the relative concentration of CO distributions from the vehicular exhaust plume along the streamwise, x, lateral,

Table 1
Measured values at the vehicular exhaust tailpipe exit and ambient conditions

Diesel vehicle	Tailpipe diameter (m)	Tailpipe height (m)	Idle condition	Exhaust exit velocity V_e ($m\,s^{-1}$)	Exhaust temperature T_e (K)	Ambient temperature T_a (K)	Exhaust CO concentration C_e (ppm)
A	0.048	0.32	Low	8.4	355.1	304.0	280
			High	22.7	488.5	302.0	385
B	0.054	0.37	Low	15.2	341.4	303.0	119
			High	24.5	548.0	303.4	435

y, and transversal, z, directions were only within 10, 8 and 4 m, respectively. Hence, a WDFW approach was used to obtain the real pollutant concentration dispersion along with the development of a vehicular exhaust plume. In order to optimise the computational costs in terms of time and storage data, and the large amount of input boundary data for simulating the three-dimensional vehicular pollutant dispersion problem, the local arbitrary wind magnitude and direction within the specified sampling period were transformed into the four major corresponding directions (i.e., N, E, S or W) and was input as one of the corresponding inflow boundary conditions in the present study. In Fig. 2, the magnitude and direction of wind, u_P, with respect to an arbitrary wind angle, α, for $0<\alpha<\pi/2$ can then be transformed into

$$u_S = u_P \cos\alpha \quad \text{and} \quad u_W = u_P \sin\alpha, \tag{1}$$

where u_P is the measured wind velocity in direction OP, and u_S and u_W are the transformations of wind velocity instantaneously from u_P into the directions S and W, respectively. Similarly, the magnitude and direction of wind with respect to an arbitrary wind angle for $\pi/2\leqslant\alpha\leqslant\pi$, $\pi<\alpha<3\pi/2$ and $3\pi/2\leqslant\alpha\leqslant2\pi$ can also be transformed into its corresponding N, E, S or W direction.

The frequency of the transformed wind direction is then defined as

$$F_i = \frac{N_i}{\sum_i\sum_j N_{ij}}, \tag{2}$$

where F_i is the frequency of wind direction in the ith direction coordinate, $i = 1$, 2, 3 and 4 represent the N, E, S and W directions, respectively, N_i is the number of times corresponding to the ith direction coordinate, and N_{ij} is the number of times in respect to the corresponding ith direction coordinate for the specified sampling period, j.

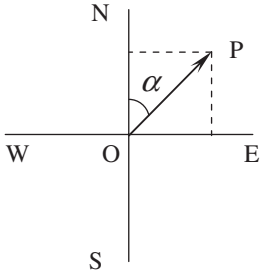

Fig. 2. Transformation of wind direction.

The averaged ambient wind velocity is defined as

$$U_i = \frac{\sum_i u_i}{N_i}, \tag{3}$$

where U_i is the averaged ambient wind velocity in the corresponding ith direction coordinate and u_i is the instantaneous ambient wind velocity in the corresponding ith direction coordinate. Once the ambient wind velocities and directions during the specified sampling period are transformed and summed up, the frequency of ambient wind directions and the averaged magnitude of ambient wind velocities can be calculated. It is obvious that the total frequency of wind in the four directions during the specified sampling period should be 100%. Table 2 shows the frequency of corresponding ambient wind directions and the averaged magnitude of ambient wind velocity during the specified sampling period at the height of 1.5 m above the ground for vehicles A and B at low and high idle conditions. Based on the WDFW approach for the real atmospheric environment, the averaged pollutant concentration during the specified sampling period can then be defined as

$$C = \sum_i F_i C_i, \tag{4}$$

where F_i and C_i are the obtained frequencies of ambient wind direction and the simulated pollutant concentration within the computational domain under the averaged ambient wind velocity in the corresponding N, E, S or W directions, respectively.

3.2. Governing equations and numerical solvers

In general, vehicular pollutants are emitted from an exhaust tailpipe at a certain flow rate, then they mix with air and disperse along three directions into the atmosphere as shown in Fig. 1. Considering the three-dimensional steady flow problem in Fig. 1, the governing equations are described as follows:

Continuity equation:

$$\frac{\partial\rho u_i}{\partial x_i} = 0. \tag{5}$$

Momentum equation:

$$\frac{\partial u_i}{\partial t} + u_j\frac{\partial\rho u_i}{\partial x_j} = -\frac{\partial p}{\partial x_i} + \frac{\partial}{\partial x_j}\left[\mu\left(\frac{\partial u_j}{\partial x_i}+\frac{\partial u_i}{\partial x_j}\right) - \rho u_i' u_j'\right] + g_i(\rho-\rho_0), \tag{6}$$

Table 2
Corresponding boundary conditions of the vehicular exhaust pollutant dispersion model

Parameter	Inflow	Inlet	Outflow	Symmetry	Ground
Velocity	Specified profile: U_z	Constant: V_e	Zero gradient	Zero gradient	No slip condition
Temperature	Constant: T_a	Constant: T_e	Zero gradient	Zero gradient	Zero gradient
Concentration	Constant: C_b	Constant: C_e	Zero gradient	Zero gradient	Zero gradient

where

$$-\rho_j u_i' u_j' = \mu_t\left(\frac{\partial u_i}{\partial x_j}+\frac{\partial u_j}{\partial x_i}\right)-\frac{2}{3}\rho k\delta_{ij}. \quad (7)$$

k and ε transport equations in the standard k–ε turbulence model:

$$\frac{\partial k}{\partial t}+\frac{\partial(\rho k u_i)}{\partial x_i} = \frac{\partial}{\partial x_j}\left[\left(\mu+\frac{\mu_t}{\sigma_k}\right)\frac{\partial k}{\partial x_j}\right]+G_k+G_b-\rho\varepsilon, \quad (8)$$

$$\frac{\partial \varepsilon}{\partial t}+\frac{\partial(\rho\varepsilon u_i)}{\partial x_i} = \frac{\partial}{\partial x_j}\left[\left(\mu+\frac{\mu_t}{\sigma_\varepsilon}\right)\frac{\partial \varepsilon}{\partial x_j}\right] + C_{1\varepsilon}\frac{\varepsilon}{k}(G_k+C_{3\varepsilon}G_b)-\rho C_{2\varepsilon}\frac{\varepsilon^2}{k}, \quad (9)$$

where

$$G_b=\beta g_i\frac{\mu_t}{Pr_t}\frac{\partial T}{\partial x_i}, \quad (10)$$

$$\beta=-\frac{1}{\rho}\left(\frac{\partial\rho}{\partial T}\right)_p, \quad (11)$$

$$G_k=\mu_t\frac{\partial u_j}{\partial x_i}\left(\frac{\partial u_i}{\partial x_j}+\frac{\partial u_j}{\partial x_i}\right). \quad (12)$$

The species (pollutants) transport and energy equations

$$\frac{\partial\rho h}{\partial t}+\frac{\partial\rho u_i h}{\partial x_i} = \frac{\partial}{\partial x_i}\left(\left(k_i+\frac{\mu_t}{Pr_t}\right)\frac{\partial T}{\partial x_i}\right) -\frac{\partial}{\partial x_i}\sum_j(h_j J_i)+\frac{Dp}{Dt}+\tau_{ik}\frac{\partial u_i}{\partial x_k}, \quad (13)$$

$$\frac{\partial\rho C_i}{\partial t}+\frac{\partial\rho u_i C_i}{\partial x_i}=\frac{\partial}{\partial x_i}\left(\rho D_{i,m}+\frac{\mu_t}{Sc_t}\right)\frac{\partial C_i}{\partial x_i}, \quad (14)$$

where $-u_i'u_j'$ is the Reynolds stress, ρ is the fluid density, u_i and u_j are the mean velocity components in ith and jth direction coordinates, respectively, p is the pressure, $\mu_t=\rho C_\mu k^2/\varepsilon$ is the turbulent viscosity, μ is the laminar viscosity, g_i is the gravitational acceleration in the ith direction coordinate, (0,0,−g), σ_k and σ_ε are the turbulent Prandtl numbers for k and ε, respectively, G_k is the generation of turbulence kinetic energy due to the mean velocity gradients, G_b is the generation of turbulence kinetic energy due to buoyancy, β is the coefficient of thermal expansion, empirical constants of $C_{1\varepsilon}$, $C_{2\varepsilon}$, $C_{3\varepsilon}$, C_μ, σ_k and σ_ε for the standard k–ε turbulence model are 1.44, 1.92, 1.44, 0.09, 1.0 and 1.3, respectively, C_i is the mean chemical species (pollutants) concentration, T is the temperature, Pr_t is the turbulent Prandtl number, 0.85, Sc_t is the turbulent Schmidt number, 0.7, h is the static enthalpy, k_i is the molecular conductivity, J_i is the diffusion flux of the ith species due to the concentration gradients, τ_{ik} is the deviatoric stress tensor, and $D_{i,m}$ is the diffusion coefficient for ith species in the mixture. Based on the present experimental set-up in an open environmental area, a horizontal homogeneous meteorology was used. Vehicle movement, the vehicle- and building-induced turbulence were not taken into account in the numerical simulation.

Fig. 3 shows the three-dimensional computational domain behind a vehicular exhaust tailpipe. The simulated physical domain is 10 m long, 8 m wide and 4 m high. Fine meshes were used near the exit of the vehicular exhaust tailpipe. Extensive tests of the independence of the meshes were carried out with increasing mesh numbers until further refinement is shown to be less significant. Mixed hexahedral and tetrahedral meshes used for the present calculation were about 250,000 in order to cover the computational domain. The computational domain for the vehicular exhaust pollutant on near-field dispersion is shown in Fig. 3. One of the inflow boundary conditions is the local ambient wind with specified velocity and direction and another inlet boundary condition is the vehicular exhaust jet plume from the tailpipe exit. The

symmetrical boundaries and the solid boundary are the top and both sides of the computational domain (i.e., parallel to the windflow direction) and the ground face, respectively. The local arbitrary wind magnitude and direction within the specified sampling period were transformed into the four major corresponding directions (i.e., N, E, S or W). The corresponding boundary conditions of a vehicular exhaust pollutant dispersion model are shown in Fig. 4 and listed in Table 2.

A power law for the profile of wind velocity was used to describe the fully developed vertical profile of the horizontal wind velocity under a neutral stability condition as follows:

$$\frac{U_z}{U_{\text{ref}}} = \left(\frac{z}{z_{\text{ref}}}\right)^p, \tag{15}$$

where U_z and U_{ref} are the mean wind velocities at the heights of z and z_{ref}, respectively, z and z_{ref} are the specified and reference (1.5 m) heights, respectively, and p is the vertical wind profile power index, 0.25. In the present study, U_{ref} is equal to U_i at $z_{\text{ref}} = 1.5$ m, as shown in Table 3.

The initial conditions were given according to the ambient and vehicle exhaust jet conditions for the present computational study. All calculations were performed using second-order accurate upwind schemes. The well-known SIMPLE algorithm was used for solving the applied numerical model. The segregated, implicit and steady solvers were set to obtain the numerical results based on the simultaneous under-relaxation factors, convergence criterion and iteration numbers. All these settings and calculations were carried out by the operation environment of commercial FLUENT code except the final averaged pollutant concentration from Eq. (4).

The relative concentration (R_C) of carbon monoxide is defined (Kim et al., 2001) as follows:

$$R_C = \frac{C_k - C_b}{C_e - C_b}, \tag{16}$$

where C_k is the simulated concentration at the specified point k.

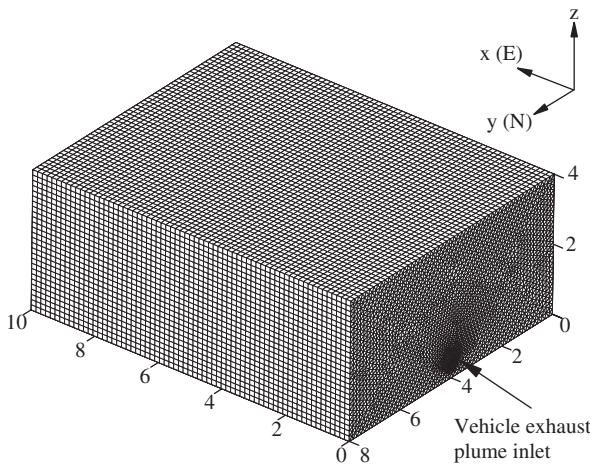

Fig. 3. Geometry and mesh of computational domain.

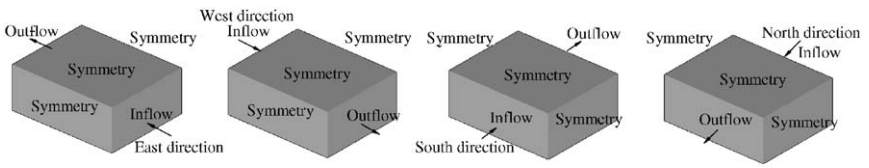

Fig. 4. Boundary conditions of a vehicular exhaust pollutant dispersion model for different ambient wind directions.

Table 3
Transformation of ambient wind directions and velocities for vehicles A and B under low and high idle conditions

Wind direction	Low idle condition				High idle condition			
	Vehicle A		Vehicle B		Vehicle A		Vehicle B	
	F_i	U_i (m s^{-1})	F_i	U_i (m s^{-1})	F_i	U_i (m s^{-1})	F_i	U_i (m s^{-1})
N	0.250	0.871	0.250	0.900	0.111	0.630	0.333	0.886
E	0.458	1.017	0.354	1.236	0.167	1.479	0.139	0.860
S	0.250	0.665	0.250	0.876	0.389	0.844	0.167	1.085
W	0.042	0.426	0.146	0.917	0.333	1.057	0.361	1.053

4. Results and discussion

4.1. Calculated results for different ambient windflow conditions using the WDFW approach

Fig. 5 shows the calculated relative CO concentration, R_C, distributions of a vehicular exhaust plume at $y = 4$ m along the streamwise, x, and transversal, z, directions for vehicle A under the low idle condition using different ambient wind directions and the WDFW approach. It shows clearly that the pollutant concentration dispersion process in the atmosphere from a vehicular exhaust plume along the streamwise distance is highly dependent on the corresponding frequencies of wind directions and magnitudes of wind velocities as shown in Table 3. When the ambient wind flows from direction E (i.e., an opposite flow direction of the vehicular exhaust plume), the exhaust plume is dispersed closer to the vehicle tailpipe exit along the streamwise distance due to the reversed flow resistance, but is dispersed further in the transversal distance, as shown in Fig. 5(a). On the other hand, the vehicular exhaust plume is dispersed further along the streamwise distance, but is dispersed closer to the vehicle tailpipe exit in the transversal distance when the ambient wind flows from direction W (i.e., the same flow direction of the vehicular exhaust plume), as shown in Fig. 5(c). In Table 3, the frequencies of ambient windflows from directions S and N (i.e., the flow direction perpendicular to the exit flow of vehicular exhaust plume) are the same ($F_i = 0.250$) and the magnitude of wind velocities is only slightly different (in S direction, $U_i = 0.871\,\mathrm{m\,s^{-1}}$, and in N direction, $U_i = 0.665\,\mathrm{m\,s^{-1}}$). Hence, the magnitude of pollutant concentration distributions of CO should be quite similar, as shown in Figs. 5(b) and (d). Fig. 5(e) shows that the relative concentration distributions of CO along the streamwise and transversal distances of a vehicular exhaust plume using the WDFW approach is similar in shape to Fig. 5(a). The relative concentrations show the influence of the combined effect and weight of the mean wind velocities and frequencies in all the considered directions. This is because the frequency of ambient windflows in E direction, $F_i = 0.458$, is 10 times more than the frequency of ambient windflows from direction W, $F_i = 0.042$, and the averaged ambient wind velocity from direction E, $U_i = 1.017\,\mathrm{m\,s^{-1}}$, is also relatively higher than the averaged ambient wind velocity from direction W, $U_i = 0.426\,\mathrm{m\,s^{-1}}$. The values from directions S and N have already been mentioned.

Fig. 6 shows the calculated relative CO concentration, R_C, distributions of a vehicular exhaust plume at $z = 0.32$ m along the streamwise, x, and lateral, y, directions for vehicle A under the low idle condition using different ambient wind directions and the WDFW approach. It also shows clearly the impact of the frequencies of wind directions and magnitudes of wind velocities on the pollutant concentration dispersion process in the atmosphere from a vehicular exhaust plume along the lateral distance. If the ambient windflows are dominant from direction E, the vehicular exhaust plume is dispersed closer to the vehicle tailpipe exit along the streamwise distance due to the reversed flow resistance, but is dispersed further along the lateral distance, as shown in Fig. 6(a) and vice versa in Fig. 6(c). In Figs. 6(b) and (d), the vehicular exhaust plumes are dispersed further along the lateral distance in the opposite way if the corresponding ambient wind flows from direction S or N. Again, a similar vehicular pollutant concentration dispersion pattern along the lateral distance is observed because the frequencies of ambient windflows from directions S and N are equal, as shown in Table 3. Fig. 6(e) shows the relative CO concentration distributions of a vehicular exhaust plume along the streamwise and lateral distances using the WDFW approach. The vehicular exhaust plume is dispersed closer along the streamwise distance, but is dispersed almost equally along the lateral distance.

Figs. 7–10 show the calculated relative CO concentration, R_C, distributions of a vehicular exhaust plume at $z = 0.32$ and 0.37 m along the streamwise, x, and lateral, y, directions for vehicles A and B under low and high idle conditions using the WDFW approach. It is observed again that the pollutant concentration dispersion process in the atmosphere depends on the frequencies of wind directions and magnitudes of wind velocities from a vehicular exhaust plume along the streamwise, x, and lateral, y, distances. From Fig. 7, the vehicular exhaust plume is dispersed closer along the streamwise distance, but is dispersed almost equally along the lateral distance. In Fig. 8, the dispersion of the vehicular exhaust plume from vehicle A under a high idle condition is enhanced along the streamwise distance at which $R_C = 0.02$ (or 2%) at $x = 2.2$ m, but is slightly toward the directions N and E along the lateral distance. This is because the frequencies of ambient windflow, $F_i = 0.389$, from direction S and $F_i = 0.333$ from direction W are much higher than the frequencies of ambient windflows from direction N, $F_i = 0.111$,

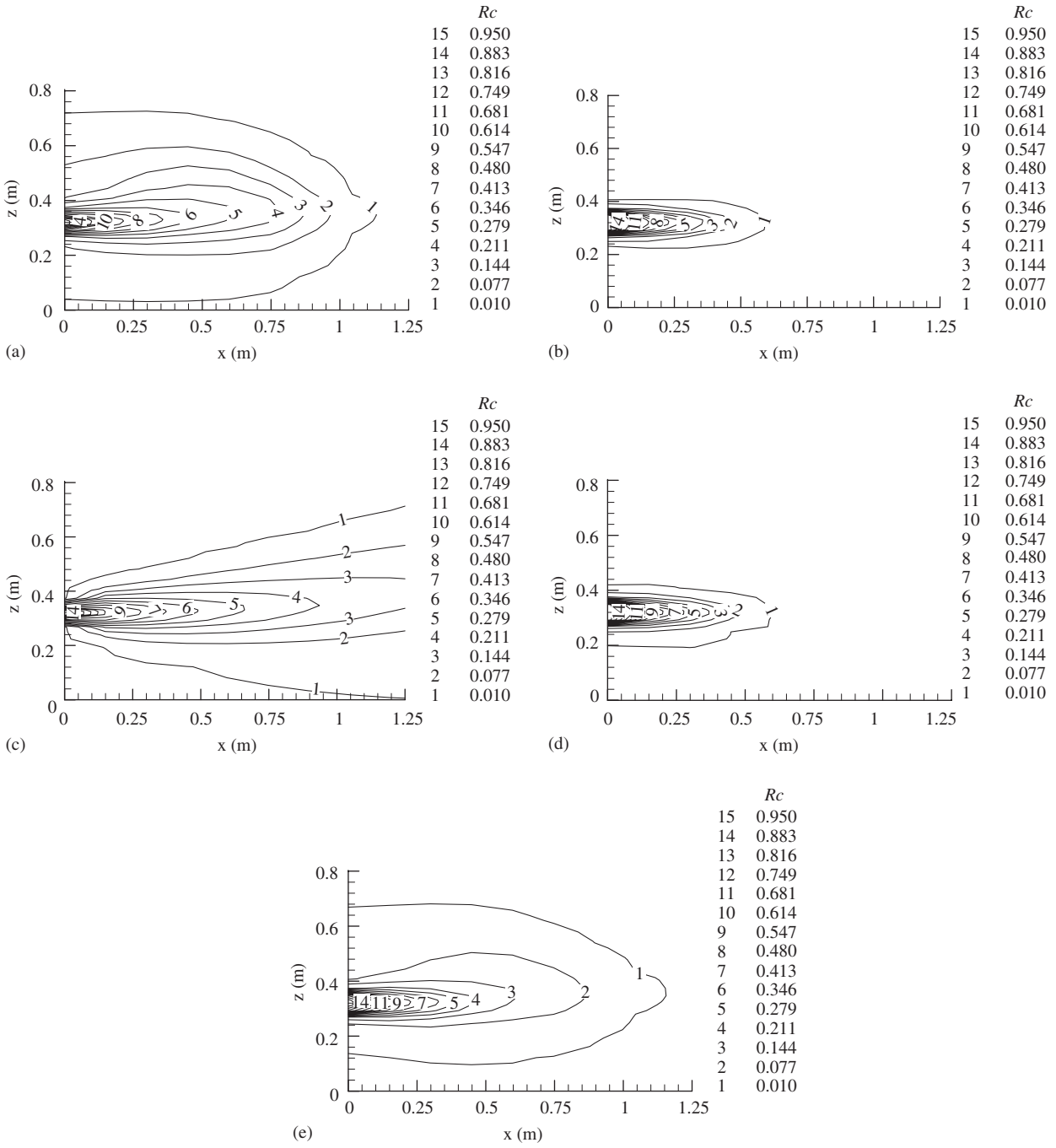

Fig. 5. Relative concentration, R_C, of CO distributions on x–z plane along the streamwise distance of a vehicular exhaust plume at $y = 4$ m for vehicle A under a low idle and different ambient windflow conditions: (a) E direction, (b) S direction, (c) W direction, (d) N direction and (e) WDFW approach used.

and from direction E, $F_i = 0.167$, and the averaged ambient wind velocities from direction S, $U_i = 0.844\,\mathrm{m\,s^{-1}}$, and $U_i = 1.479\,\mathrm{m\,s^{-1}}$, from direction E are also slightly higher than the averaged ambient wind velocities, $U_i = 0.630\,\mathrm{m\,s^{-1}}$, from direction N and $U_i = 1.057\,\mathrm{m\,s^{-1}}$ from direction W, as shown in Table 3. On the other hand, the dispersion process of a vehicular exhaust plume for vehicle A at a low idle condition is reduced along the streamwise distance at which $R_C = 0.02$ (or 2%) at $x = 1.1$ m,

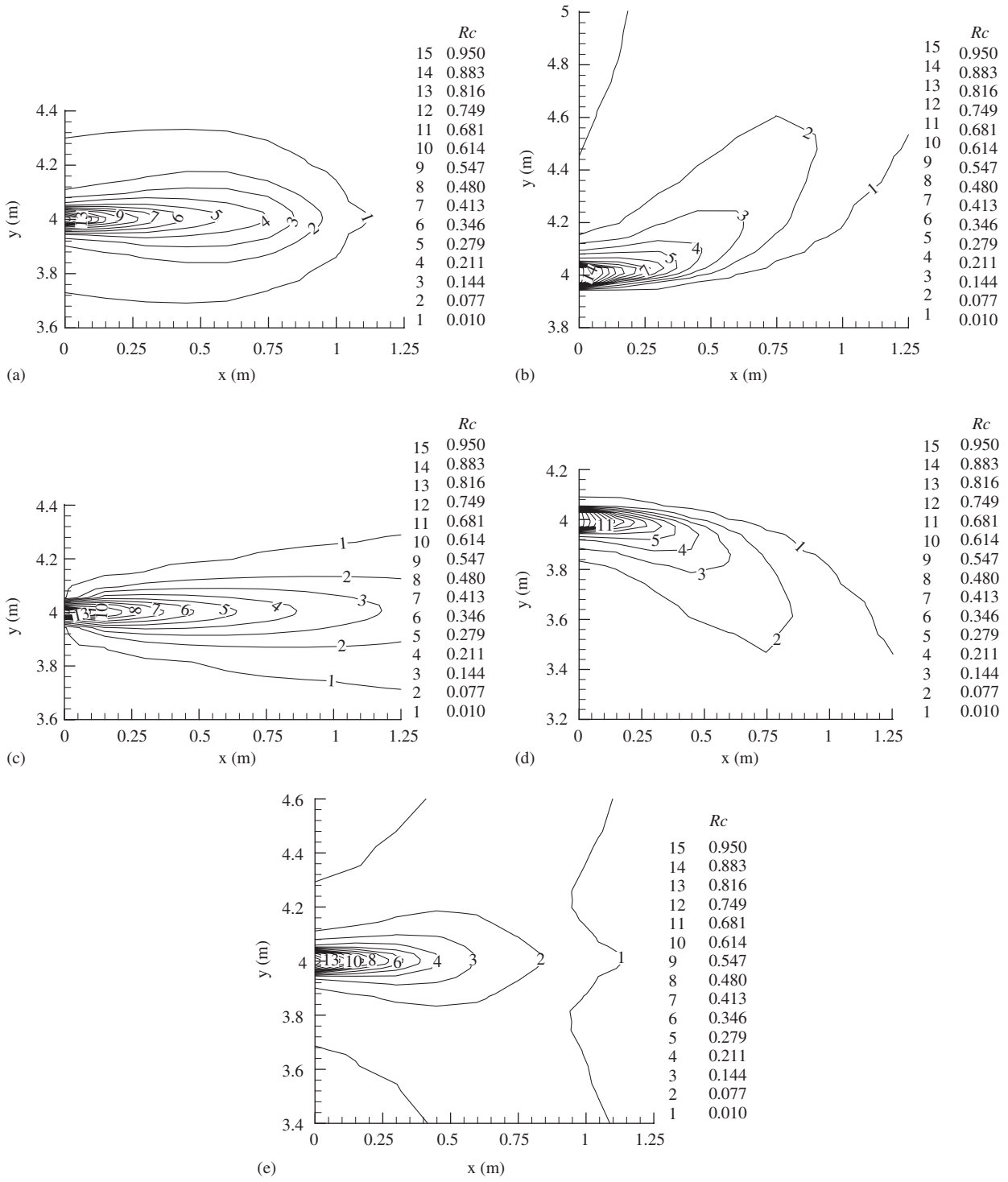

Fig. 6. Relative concentration, R_C, of CO distributions on x–y plane along the streamwise distance of a vehicular exhaust plume at $z = 0.32$ m for vehicle A under a low idle and different ambient windflow conditions: (a) E direction, (b) S direction, (c) W direction, (d) N direction and (e) WDFW approach used.

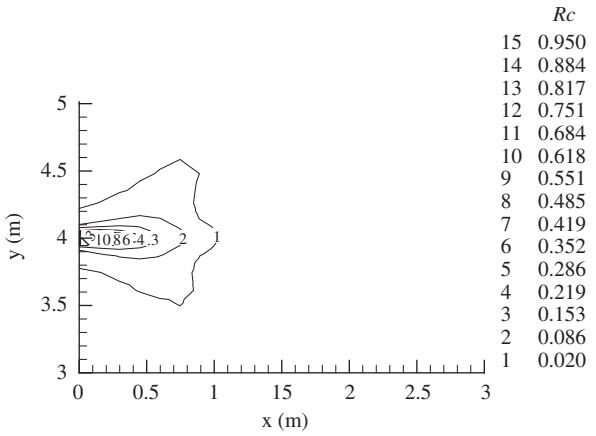

Fig. 7. Relative concentration, R_C, of CO distributions on x–y plane along the streamwise distance of a vehicular exhaust plume at $z = 0.32$ m for vehicle A under a low idle condition using the WDFW approach.

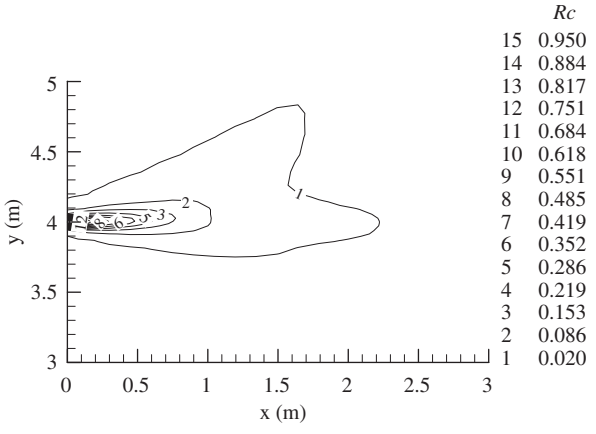

Fig. 8. Relative concentration, R_C, of CO distributions on x–y plane along the streamwise distance of a vehicular exhaust plume at $z = 0.32$ m for vehicle A under a high idle condition using the WDFW approach.

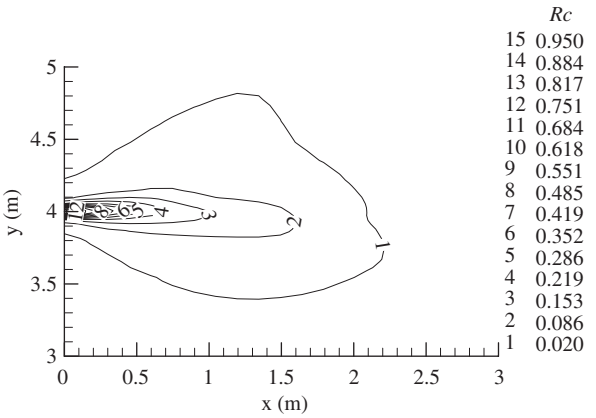

Fig. 9. Relative concentration, R_C, of CO distributions on x–y plane along the streamwise distance of a vehicular exhaust plume at $z = 0.37$ m for vehicle B under a low idle condition using the WDFW approach.

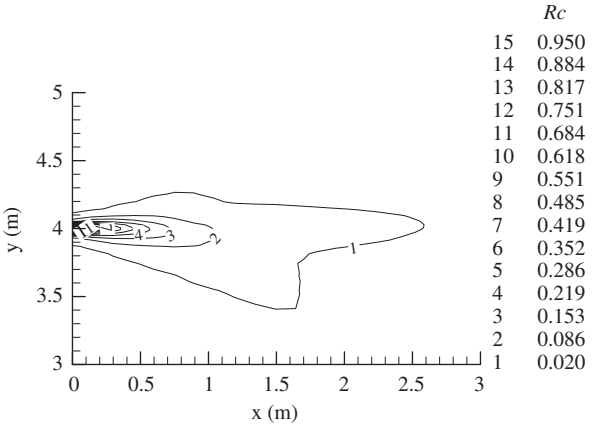

Fig. 10. Relative concentration, R_C, of CO distributions on x–y plane along the streamwise distance of a vehicular exhaust plume at $z = 0.37$ m for vehicle B under a high idle condition using the WDFW approach.

but is equally distributed to both directions S and N along the lateral distance, as shown in Fig. 7. This is due to different wind velocities and directions occurring under this sampling period. Similarly, the dispersion of the vehicular exhaust plume from vehicle B at a low idle condition is enhanced along the streamwise distance at which $R_C = 0.02$ (or 2%) at $x = 2.2$ m, but is almost equally distributed to both S and N directions along the lateral distance, as shown in Fig. 9. This is because the frequency of ambient windflows from direction E, $F_i = 0.458$, is 10 times greater than $F_i = 0.042$ from direction W, and the averaged ambient wind velocity from direction E, $U_i = 1.017\,\mathrm{m\,s^{-1}}$, is 2 times higher than the averaged ambient wind velocity from direction W, $U_i = 0.426\,\mathrm{m\,s^{-1}}$. In addition, the frequency of ambient windflow conditions from directions S and N are equal to $F_i = 0.25$, and the averaged ambient wind velocity from direction S, $U_i = 0.665\,\mathrm{m\,s^{-1}}$, is only slightly lower than the averaged ambient wind velocity from direction N, $U_i = 0.871\,\mathrm{m\,s^{-1}}$. On the other hand, the exhaust plume of vehicle B at a high idle condition is dispersed rapidly along the streamwise distance at which $R_C = 0.02$ (or 2%) at $x = 2.6$ m, but is slightly toward the directions S and E along the lateral

distance, as shown in Fig. 10. The details of individual frequencies of ambient windflow direction and velocities are presented in Table 3.

From these calculated results, it is also found that the effect of vehicular exhaust exit velocity on the dispersion process is more significant than that of ambient wind velocity in the vicinity of the exhaust tailpipe exit, while the effect of ambient wind velocity gradually shows a significant role in the dispersion process in the periphery of the vehicular exhaust plume. The present study shows that the pollutant concentration dispersion process is less influenced by the ambient wind velocity in the near region for $R_C = 0.1$–1 (or 10–100%), than by the vehicular exhaust exit velocity, but it is vice versa in the far region for $R_C = 0$–0.1 (or 0–10%).

4.2. Effect on pollutant concentration dispersion using the WDFW approach

To validate the developed three-dimensional numerical model coupled with a k–ε turbulence model and the WDFW approach, two diesel-fuelled vehicles, A and B, were used to obtain the CO concentration distributions of a vehicular exhaust plume. Figs. 11–18 show the comparison between the measured and calculated relative concentrations of CO of a vehicular exhaust plume in x–z and y–z planes for both vehicles. The results show a good prediction using the present three-dimensional numerical model coupled with the WDFW approach. In Figs. 11 and 15, the relative concentrations of CO decrease exponentially along the centreline of the vehicular exhaust plume for different idle conditions due to the initial dispersion process. The relative pollutant concentrations reduce rapidly close to ambient concentration values in a short streamwise distance of 4 m. In Figs. 12 and 16, the relative concentrations of CO at 1.5 m above ground level mix rapidly with the surrounding ambient air along the lateral distance. The relative pollutant concentration at location 7 is found to be slightly higher than at location 1. It implies that the combined effects of entrainment and buoyancy of the vehicular exhaust thermal plume have taken place with the surrounding ambient air. Details on heat transfer and flow characteristics of a thermal jet can be found in Chan et al. (2002b). In Figs. 13 and 17, the relative concentrations of CO at 1.5 m above ground decrease with increasing lateral distances from location 2 for different idle conditions. The symmetric relative pollutant concentration distributions for a low idle condition in both vehicles are due to similarities between the frequencies of wind in the N and S directions and their velocities as shown in Table 3. On the other hand, the less symmetric relative pollutant concentration distributions for a

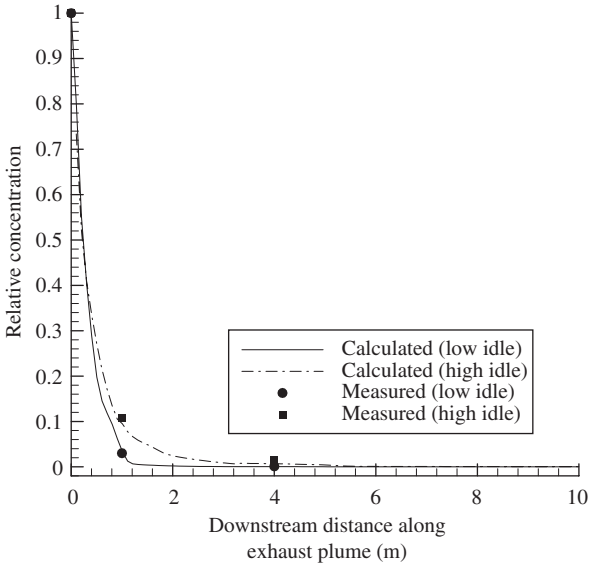

Fig. 11. Comparison of relative concentration, R_C, between the measured and calculated CO data (at points 0, 2 and 8) of a vehicular exhaust plume at $z = 0.32$ m for vehicle A under high and low idle conditions using the WDFW approach.

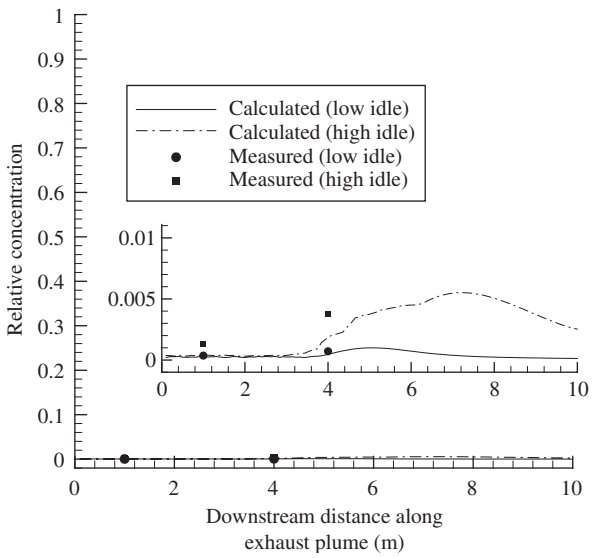

Fig. 12. Comparison of relative concentration, R_C, of CO between the measured and calculated CO data (at points 1 and 7) of a vehicular exhaust plume at $z = 1.5$ m for vehicle A under high and low idle conditions using the WDFW approach.

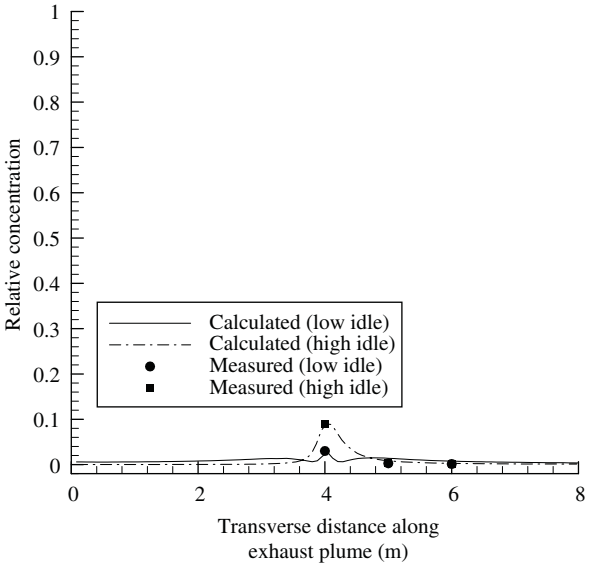

Fig. 13. Comparison of relative concentration, R_C, of CO between the measured and calculated data (at points 2, 4 and 6) of a vehicular exhaust plume at $z = 0.32$ m for vehicle A under high and low idle conditions using the WDFW approach.

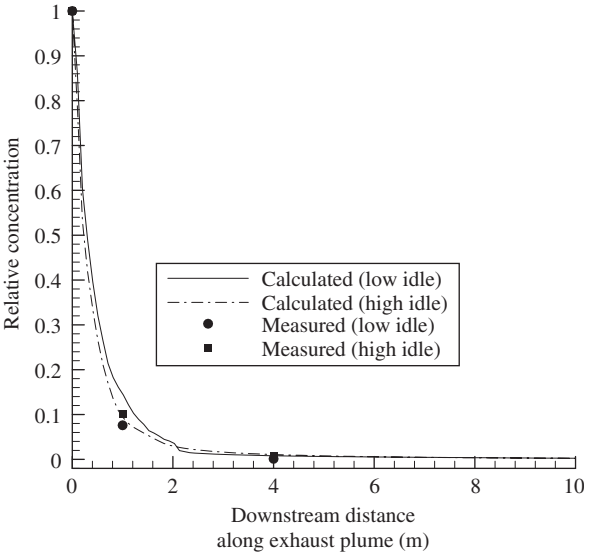

Fig. 15. Comparison of relative concentration, R_C, of CO between the measured and calculated data (at points 0, 2 and 8) of a vehicular exhaust plume at $z = 0.37$ m for vehicle B under high and low idle conditions using the WDFW approach.

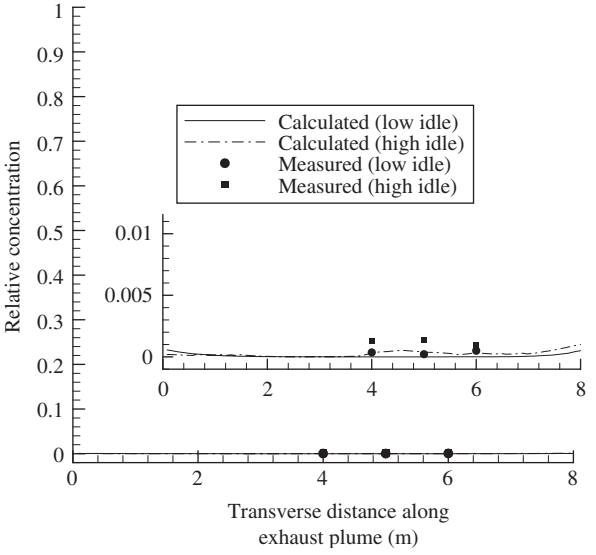

Fig. 14. Comparison of relative concentration, R_C, of CO between the measured and calculated data (at points 1, 3 and 5) of a vehicular exhaust plume at $z = 1.5$ m for vehicle A under high and low idle conditions using the WDFW approach.

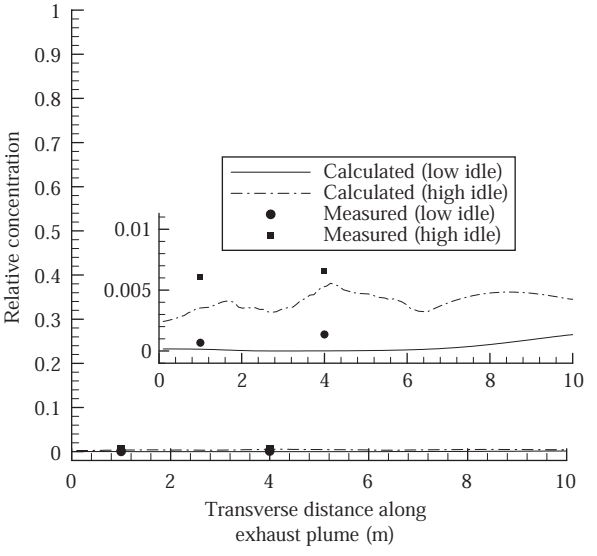

Fig. 16. Comparison of relative concentration, R_C, of CO between the measured and calculated data (at points 1 and 7) of a vehicular exhaust plume at $z = 1.5$ m for vehicle B under high and low idle conditions using the WDFW approach.

high idle condition in both vehicles result from the fact that the frequency of wind in N and S directions is quite different and their wind velocities are also slightly different from each other. In Figs. 8 and 10, the effects of wind direction and velocity on the vehicular pollutant concentration dispersion are in N and S directions, respectively. Here, more realistic qualitative features of airflow and pollutant concentrations of the vehicular exhaust plume in near-field scale can be reproduced using the developed three-dimensional numerical model coupled with a k–ε turbulence model and the WDFW approach. In

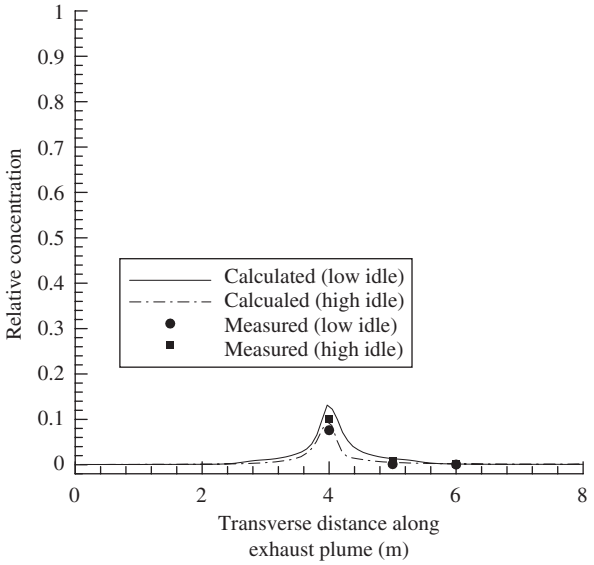

Fig. 17. Comparison of relative concentration, R_C, of CO between the measured and calculated data (at points 2, 4 and 6) of a vehicular exhaust plume at $z = 0.37$ m for vehicle B under high and low idle conditions using the WDFW approach.

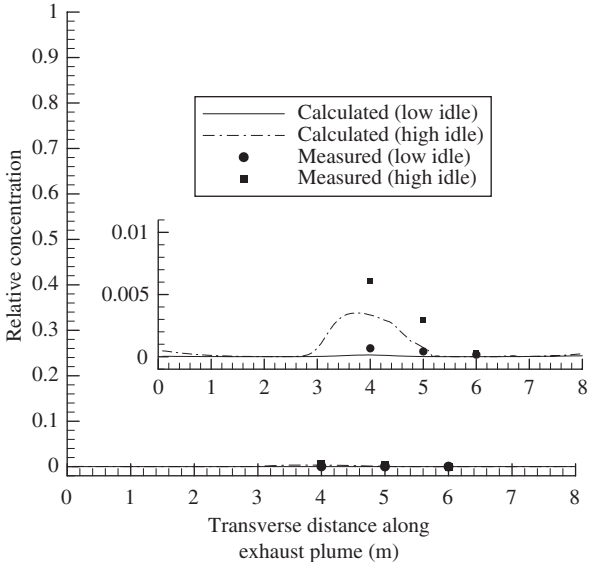

Fig. 18. Comparison of relative concentration, R_C, of CO between the measured and calculated data (at points 1, 3 and 5) of a vehicular exhaust plume at $z = 1.5$ m for vehicle B under high and low idle conditions using the WDFW approach.

Figs. 14 and 18, the relative concentrations of CO above the ground level of 1.5 m decrease with increasing lateral distance from the exhaust tailpipe exit at location 1 for different idle conditions.

In general, good agreement between the calculated and measured data for two diesel-fuelled vehicles demonstrates that the developed three-dimensional vehicular pollutant dispersion numerical model based on the RANS equations coupled with a k–ε turbulence model and the WDFW approach provides a good insight into the initial dispersion of pollutant concentration from a vehicular exhaust plume in the real atmospheric environment. The larger differences between the measured and calculated data are observed at location(s) 2 and/or 4 for both vehicles A and B at a low idle condition. It may be due to the effects of complex local ambient wind field in the real atmosphere, and the wake generation from the interaction between the vehicle geometry, and arbitrary ambient wind magnitude and direction on near-field vehicular exhaust plume dispersion.

5. Summary and conclusions

A three-dimensional vehicular pollutant dispersion numerical model was developed based on the Reynolds-averaged Navier–Stokes equations coupled with a k–ε turbulence model to simulate the initial pollutant dispersion process of carbon monoxide, CO, from a vehicular exhaust plume in the real atmospheric environment. Since ambient wind direction and velocity are stochastic and uncontrollable in the real atmospheric environment, a wind-direction–frequency-weighted (WDFW) approach was used to obtain the real pollutant concentration dispersion along with the development of vehicular exhaust plume. Within the specified sampling period, the local ambient windflow conditions are transformed into the corresponding frequencies of wind directions and averaged magnitude of wind velocities from directions N, E, S or W. Based on the present experimental set-up in an open environmental area, the horizontal homogeneous meteorology, vehicle movement, vehicle- and building-induced turbulence have not been taken into account in the numerical calculation. Good agreement between the calculated and measured data for two diesel-fuelled vehicles indicates that the WDFW approach can truly reflect the initial dispersion of pollutant concentration from a vehicular exhaust plume in the real atmospheric environment. The present study shows that the dispersion process in the near region for the relative concentration of CO, from $R_C = 0.1$ (or 10%) to 1 (or 100%) is less influenced by the ambient wind velocity than the vehicular exhaust exit velocity, but it is vice versa in the far region, from $R_C = 0$ (or 0%) to 0.1 (or

10%). It implies that the effect of vehicular exhaust exit velocity on the dispersion process is more pronounced than the effect of ambient wind velocity at the vicinity of the exhaust tailpipe exit, while the effect of ambient wind velocity gradually shows a significant role in the dispersion process along with the development of the vehicular exhaust plume.

Acknowledgements

This work was supported by grants from the Research Grants Council of the Hong Kong Special Administrative Region, China (RGC Project no. PolyU 5154/01E) and the Central Research Grants of The Hong Kong Polytechnic University (Project no. B-Q497).

References

Chan, T.L., Dong, G., Cheung, C.S., Leung, C.W., Wong, C.P., Hung, W.T., 2001. Monte Carlo simulation of nitrogen oxides dispersion from a vehicular exhaust plume and its sensitivity studies. Atmospheric Environment 35, 6117–6127.

Chan, T.L., Dong, G., Leung, C.W., Chung, C.S., Hung, W.T., 2002a. Validation of a two-dimensional pollutant dispersion model in an isolated street canyon. Atmospheric Environment 36, 861–872.

Chan, T.L., Leung, C.W., Jambunathan, K., Ashforth-Frost, S., Zhou, Y., Liu, M.H., 2002b. Heat transfer characteristics of a slot jet impinging on a semi-circular convex surface. International Journal of Heat and Mass Transfer 45, 993–1006.

Fraigneau, Y.C., Gonzalez, M., Coppalle, A., 1995. Dispersion and chemical-reaction of a pollutant near a motorway. Science of the Total Environment 169, 83–91.

Kim, D.H., Gautam, M., Gera, D., 2001. On the prediction of concentration variations in a dispersing heavy-duty truck exhaust plume using k–ε turbulence closure. Atmospheric Environment 35, 5267–5275.

Marmur, A., Mamane, Y., 2003. Comparison and evaluation of several mobile-source and line source models in Israel. Transportation Research Part D 8, 249–265.

Niemeier, U., Schlunzen, K.H., 1993. Modelling steep terrain influences on flow patterns at the Isle of Helgoland. Beitraege zur Physik der Atmosphare 66, 45–62.

Sharma, P., Khare, M., 2001. Modelling of vehicular exhausts—a review. Transportation Research Part D 6, 179–198.

Vardoulakis, S., Fisher, B.E.A., Pericleous, K., Gonzalez-Flesca, N., 2003. Modelling air quality in street canyons: a review. Atmospheric Environment 37, 155–182.

Venkatram, A., Fitz, D., Bumiller, K., Du, S.M., Boeck, M., Ganguly, C., 1999. Using a dispersion model to estimate emission rates of particulate matter from paved road. Atmospheric Environment 33, 1093–1102.